Retardation of Ice Crystallization by Short Peptides[†]

Jun Soo Kim

Department of Chemistry, University of Wisconsin, Madison, Wisconsin, 53706

Srinivasan Damodaran

Department of Food Science, University of Wisconsin, Madison, Wisconsin, 53706

Arun Yethiraj*

Theoretical Chemistry Institute and Department of Chemistry, University of Wisconsin, Madison, Wisconsin, 53706

Received: December 15, 2008; Revised Manuscript Received: February 16, 2009

The effect of peptides on the growth of ice crystals are studied using molecular dynamics simulations. The growth of the ice crystal is simulated at a supercooling of 14 K, and the effect of a single tetrapeptide on the growth rate is calculated. For pure ice the simulated crystal grows at a rate comparable to experiment. When a peptide molecule is added near the interface, the growth rate is diminished significantly, by up to a factor of 5 for Gly-Pro-Ala-Gly and a factor of 3 for Gly-Gly-Ala-Gly. The retardation occurs via the binding of the peptide to the ice surface, suppression of ice growth near the binding site, and eventual growth of the crystal around the bound peptide. The peptide with a proline residue is more effective in retarding the crystal growth, and this can be understood from the conformation of the peptide within the frozen ice phase after overgrowth. The simulations suggest that short peptides can be effective antifreeze agents.

Introduction

Antifreeze proteins are critical for the survival of organisms, such as arctic fishes, insects, and plants, that live at subzero temperatures.[1−6] The inhibition of the recrystallization of ice in these organisms is one of the important roles of these proteins, which is critical in a freeze−thaw cycle to minimize or prevent damage to cells and tissue.[2−6] Understanding the mechanism of crystal growth retardation by antifreeze proteins is a subject of current interest. Although it is accepted that antifreeze proteins retard crystal growth by binding to the ice surface, details regarding which part of the protein binds, and how this inhibits recrystallization are still not clear.[7,8] The study of antifreeze proteins might also provide insight into the effect of proteins on the growh of other crystals, such as calcium oxalate crystals involved in kidney stones.

We are interested in the behavior of *short peptides* on the growth of ice crystals. Antifreeze proteins are too expensive for routine use, and low-cost alternatives are of interest. For example, one can envisage the application of antifreeze proteins in cryopreservation, where prevention of recrystallization during the freeze−thaw cycle could help preserve tissue and organs, and in maintaining the textural quality of frozen foods. From a fundamental standpoint, antifreeze proteins are quite large (5−30 kD) and the study of smaller molecules would aid the elucidation of the mechanism of antifreeze activity.

We study the antifreeze effect of short peptides on the growth of ice crystal using molecular dynamics simulations. The particular application of interest is the prevention of ice crystals in ice-cream stored in a freezer. Recently, the antifreeze effect of collagen hydrolysate has been proposed[9] and we therefore consider short peptides with sequences found abundantly in collagen. We consider two short peptides, Gly-Pro-Ala-Gly and Gly-Gly-Ala-Gly, and study their impact on ice crystal growth.

There have been several recent simulation studies on the growth of ice crystals,[10−13] but computational studies of antifreeze proteins have focused on the orientation and binding of the proteins on the ice/water interfaces (see ref 7 for a review). A recent nonequilibrium molecular dynamics simulation[14] demonstrated that a mutant of winter flounder antifreeze protein decreases the growth velocity of ice. Studying short peptides allows us to study many and much longer trajectories, and this sheds light not only on the kinetic inhibition by the peptide but also on the growth of ice crystals beyond bound peptides and the resulting frozen conformation of the peptide molecules.

We find that the presence of short tetrapeptides in the liquid phase retards the growth rate of the crystal to a significant extent. The suppression of crystal growth occurs in the region where the peptide binds to the surface, and in the absence of binding the growth rate is not affected. We also find that the peptide with a proline residue is more effective in retarding crystal growth, consistent with the fact that free proline amino acid is a natural cryoprotectant.[15] We speculate that the presence of the proline residue makes it more difficult to incorporate the peptide into the growing ice crystal.

The rest of this paper is organized as follows: The simulation method is presented in section 2, results are presented and discussed in section 3, and some conclusions are presented in section 4.

Simulation Method

Initial configurations are prepared in a manner similar to that used in our previous work on the melting of ice by salt.[13] Configurations of hexagonal proton-disordered ice (with 768

[†] Part of the "George C. Schatz Festschrift".

* Corresponding author. E-mail: yethiraj@chem.wisc.edu.

10.1021/jp8110748 CCC: $40.75
Published on Web 03/04/2009

molecules)[13,16] and liquid water (with 1152 molecules) are prepared separately and equilibrated. A single peptide molecule is placed in the liquid phase at a distance 1 nm away from boundary of the box in the z-direction, and the water molecules it overlaps with are removed. After further equilibration of the liquid phase including the peptide, the secondary prismatic interface of ice is placed in contact with the liquid phase so that the interface is the closest to the peptide. Possible bad contacts are removed with the steepest descent minimization. The size of the simulation cell prepared in this way is approximately 2.9, 3.1, and 6.6 nm in the x-, y-, and z-directions, respectively. The length of simulation box in the z-direction is increased to 15 nm with the water molecules in the middle of the cell. Periodic boundary conditions are then employed, and this results in a vapor phase on either side. There are therefore three (ice−vapor, ice−liquid, and liquid−vapor) interfaces in the simulation. The density of the peptides on the surface is 1.1×10^{13} molecules/cm^2 and the overall concentrations are 0.7 and 0.5 wt % for Gly-Pro-Ala-Gly and Gly-Gly-Ala-Gly, respectively.

Five different configurations are prepared for each of the three cases studied, namely, in the pure ice/water system, in the presence of a single Gly-Pro-Ala-Gly and a single Gly-Gly-Ala-Gly, and from them five different trajectories are obtained.

The system is evolved using molecular dynamics (MD) simulations, which are carried out with the GROMACS v3.3.2 program.[17,18] The equations of motion are integrated numerically using a leapfrog algorithm with a time step of 1 fs. The Berendsen coupling method[19] is used to keep the temperature at 260 K and the pressure at 1 bar, with coupling constants of 0.1 and 0.5 ps, respectively. The pressure coupling is only applied to the x- and y-directions while the length of the simulation box in the z-direction is kept constant. The SETTLE algorithm[20] is used to keep the water molecules rigid. A cutoff distance of 1 nm is used for Lennard-Jones interactions, and the particle-mesh Ewald method[21,22] is used for the long-range electrostatic interactions with the real space cutoff distance of 1 nm.

We use the TIP5P model for water[23] because it has a freezing point[24] ($T_f = 274$ K) close to the experimental value for ice I_h ($T_f = 273.15$ K). This may be compared to the freezing point in other popular water models such as the TIP4P model[25] ($T_f = 232$ K) or the SPC/E model[26] ($T_f = 215$ K). The interaction potentials for the peptides are obtained from the OPLS force field.[27,28] Simulations are performed at 260 K, which corresponds to a degree of supercooling of 14 K.

Results and Discussion

The pure ice crystal grows at a rate comparable to experiment. Figure 1 depicts the number of molecules in the ice phase as a function of time for $T = 260$ K. We use the same method as in the previous work to determine if a water molecule belongs to ice or the liquid water phase.[10,13] The growth rate is similar in all trajectories at 260 K and the entire simulation cell crystallizes within 25 ns. At temperatures of 265 and 270 K (not shown) the growth rate is a little slower and there is more variation between different trajectories. From the slope of the curve we estimate the growth rate at 260 K (a supercooling of 15 K) as 0.037 ± 0.006 molecules/ps. This can be converted to 13 ± 2 cm/s because each layer in the simulation box in the z-direction has 64 water molecules and the distance between layers is 0.22 nm on average. This is in good agreement with experiments. Bauerecker et al.[29] reported a growth rate of 12 cm/s at a supercooling of 20 K, and earlier experiments[30,31] reported

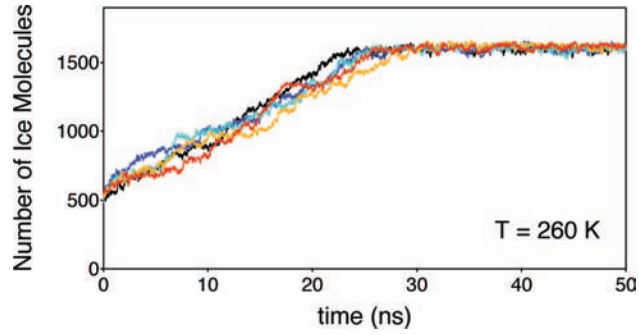

Figure 1. Increase of the number of ice molecules during crystallization at $T = 260$ K. Different colors indicate data from different trajectories.

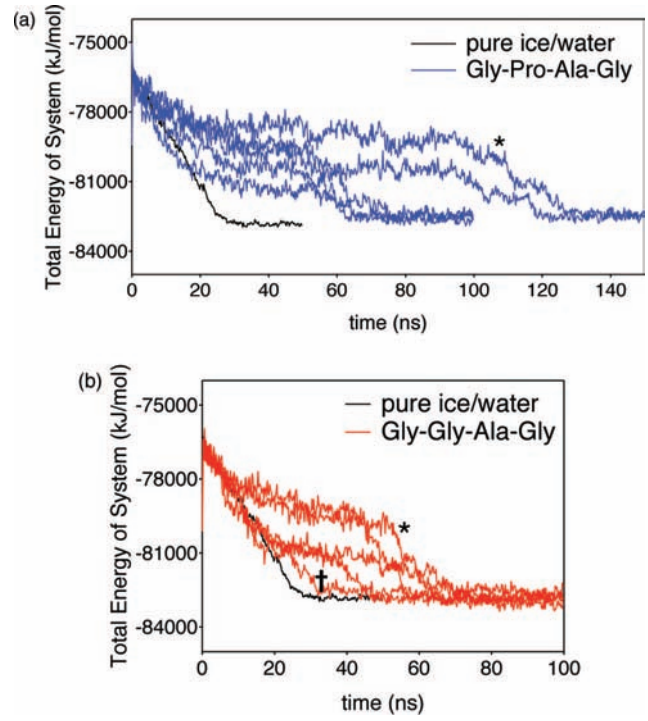

Figure 2. Total energy as a function of time with (a) Gly-Pro-Ala-Gly and (b) Gly-Gly-Ala-Gly. The black curve (shortest freezing time) is the average from five trajectories for the pure ice−water system. The symbols ★ mark the trajectories (in each case) that are most effective in retarding crystal growth, and the symbol † marks the trajectory that is least effective in retarding crystal growth.

growth rates of 6 cm/s at a supercooling of 10 K and growth rates of 8−12 cm/s at a supercooling of 18 K. These values are comparable to our growth rate of 13 ± 2 cm/s at a supercooling of 14 K. The higher growth rate in our simulations may be caused by our use of a thermostat which removes heat very efficiently.

We use the total energy of the system as a measure of the extent of crystallization, following previous work.[32] For a pure ice/water system we can assign molecules to the two different phases based on the average number of hydrogen bonds. In the presence of the peptide, however, the same criterion for the average number of hydrogen bonds is not applicable to water molecules near the peptide and an alternative measure is necessary. As the crystal grows, the thermostat removes energy from the system (because the temperature is maintained at 260 K) and the total energy decreases. Parts a and b of Figure 2 depict the total energy as a function of time for the system with Gly-Pro-Ala-Gly and Gly-Gly-Ala-Gly, respectively. Also

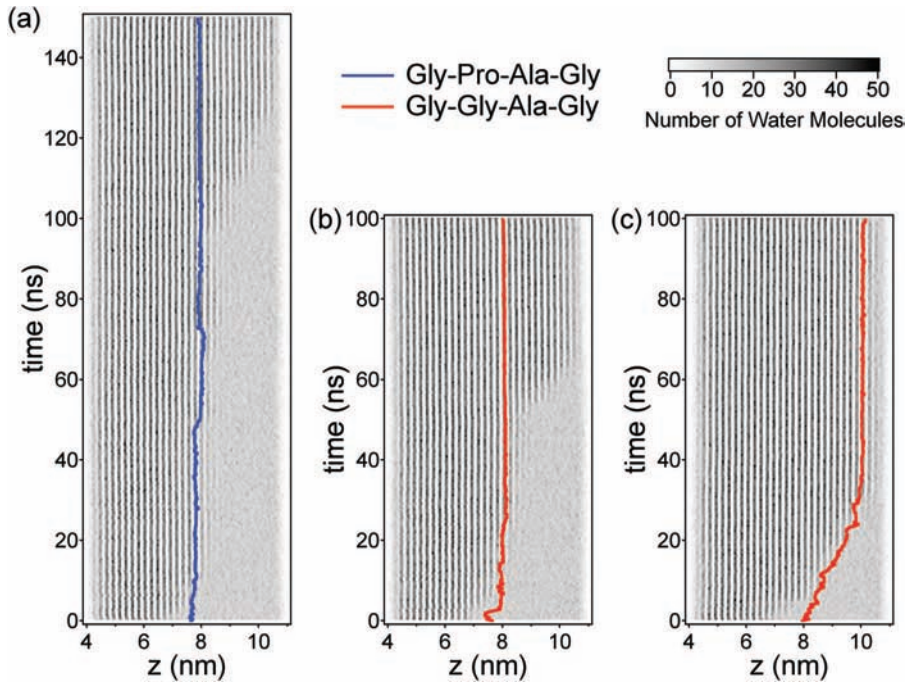

Figure 3. Time evolution of density profiles of water with traces of the center-of-mass of the peptide. (a) and (b) depict trajectories with the best activity marked by ★ in 2 with Gly-Pro-Ala-Gly and Gly-Gly-Ala-Gly, respectively, and (c) depicts the trajectory with the poorest activity marked by † in 2.

shown in the figure is the result in the absence of peptide, for which the growth rate (or freezing time) obtained in this fashion is consistent with that obtained from Figure 1.

The peptides are effective in retarding the growth of the ice crystal. For the pure ice/water mixture, the total energy reaches a plateau within 25 ns, implying that the crystallization is completed within this time. In the presence of either peptide, however, the time dependence of the total energy deviates significantly from that of pure ice/water mixture. There is considerable variation in the magnitude of the retardation between different trajectories of the same peptide. However, the retardation effect is clearly more pronounced with Gly-Pro-Ala-Gly than with Gly-Gly-Ala-Gly. Quantitatively, the growth retardation ranges from a factor of 2.5 to 5 with Gly-Pro-Ala-Gly and a factor of 1.3−3 with Gly-Gly-Ala-Gly.

The time evolution of density profiles of water molecules is useful for visualizing the growth of the crystal.[11,13] Figure 3 depicts the trajectories marked with a ★ and a † in Figure 2. In the figure, the density of water molecules is shown in grayscale with position as the x-axis and time as the y-axis. The crystal appears as a series of bands of alternating dark and light lines, and the liquid is gray. As the crystal grows, the bands start to propagate to the right. The position of the center-of-mass of the peptide is shown as the colored line. In Figure 3a, for example, the crystal−liquid interface is located at ≈7 Å at time $t = 0$, is at ≈8 Å until a time of $t = 100$ ns and then grows rapidly until the entire simulation cell is crystalline at a time of $t \approx 125$ ns.

The growth of the crystal is retarded when the peptide is bound to the interface. In Figure 3a,b, the crystal does not grow for time durations of approximately 0−100 and 0−50 ns, during which time the trace of the peptide shows that it is at the interface. At longer times the peptide is incorporated into the crystal,which then grows at a rate corresponding to that of pure water. On the other hand, in Figure 3c the trace of the peptide center-of-mass reveals that the peptide is not bound to the ice surface and pushed away from it as the ice grows. In the absence of stable binding, the growth of the crystal is not retarded significantly by the presence of the peptide near the interface. We therefore conclude that the immobilization of the peptide on the growing ice surface is required for the kinetic inhibition of crystal growth.

A series of snapshots of the trajectory in Figure 3a are shown in Figure 4. (The pictures were created using the visual molecular dynamics (VMD) program.[33]) The initial configuration (Figure 4a) has the peptide close to the interface. The peptide binds to the surface and crystal growth near the binding site (Figure 4b) is suppressed. The growth of the crystal around the peptide results in bulging ice−water interfaces between the location of periodic images of the bound peptide. Eventually the peptide is engulfed by the growing ice front and the crystal growth is completed with the peptide frozen within the crystal (Figure 4c).

The Gly-Pro-Ala-Gly peptide aligns in the direction of the crystal growth in a relatively stretched conformation, with either the N terminus or the C terminus at the interface. The difference between the z-coordinate of the N and C atoms on the terminal groups is depicted for five different trajectories in Figure 5a. At short times there are fluctuations in this quantity but in the frozen configuration this difference has approximately the same magnitude for all trajectories. Figure 5b shows that the distance between the terminal C and N atoms is roughly constant throughout all trajectories, suggesting that the peptide is stiff and the fluctuations seen in part a arise from orientational motions. Interestingly, the C terminus binds to the ice surface in four trajectories and the N terminus in one trajectory. Given the small number of trajectories, it is reasonable to conclude that the peptide can bind via either terminus. Indeed, NH_4^+ is one of the ions that is most readily accepted into the ice lattice because of its tetrahedral structure and its ionic radius similar to that of O^{2-}.[34]

We speculate the presence of the proline residue plays a crucial role in the retardation of growth. When either terminal group is stably bound to the ice surface, the presence of proline

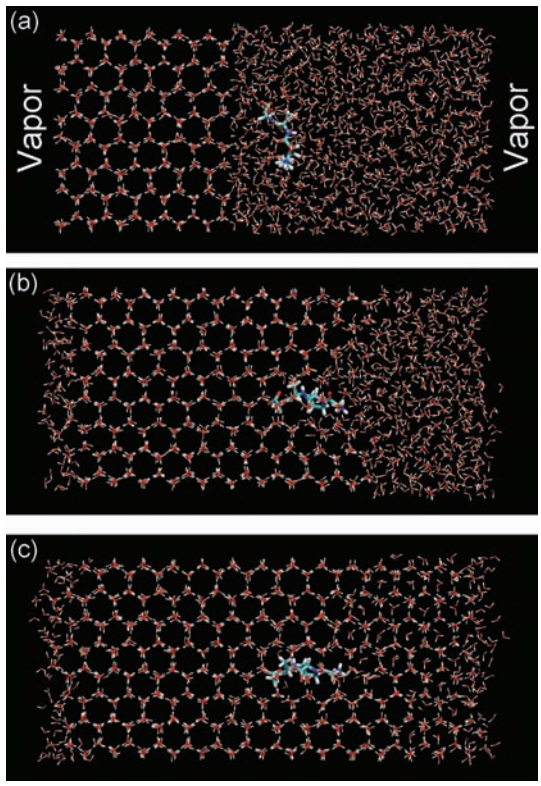

Figure 4. Snapshots from the trajectory (with Gly-Pro-Ala-Gly) marked with a ★ in Figure 2, with density profile depicted in Figure 3a for (a) the initial initial configuration of ice/peptide/water mixture sandwitched by the vapor phase on both ends, (b) the case when the peptide is bound to the ice surface and suppresses further growth of the crystal at the binding site (taken at 100 ns), and (c) $t = 150$ ns when crystallization is complete. The figure was made using the program VMD.[33]

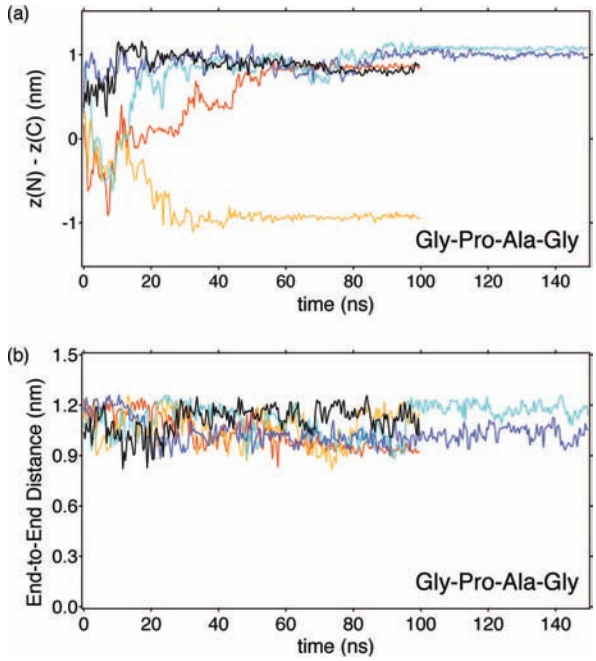

Figure 5. Conformation of the Gly-Pro-Ala-Gly peptide at the interface. (a) Difference between z-coordinates of the N atom in terminal $-NH_3^+$ and C atom in terminal $-COO^-$. Positive values imply the C-terminus is at the interface, and negative values imply the N-terminus is at the interface. (b) Distance between the N and C atoms described in (a).

residue impedes the incorporation of both the peptide itself and other water molecules into the ice crystal near the site of binding and this results in the kinetic inhibition of crystal growth.

The Gly-Gly-Ala-Gly peptide, on the other hand, shows much larger conformational fluctuations than the Gly-Pro-Ala-Gly peptide and, when incorporated into the crystal, is not in the same conformation in all trajectories. In three trajectories the peptide is stretched: parallel to the initial interface in two and at an angle in the third. In the remaining two trajectories the peptide is bent. We speculate that, because of the conformational flexibility in the binding to the ice surface, this peptide is more easily engulfed by the growing crystal front.

Conclusions

We present simulation results for the retardation of ice crystal growth by short peptides. Under a supercooling of 14 K, the growth rate is retarded by a factor of 2.5−5 by Gly-Pro-Ala-Gly and by a factor of 1.3−3 by Gly-Gly-Ala-Gly. The simulations suggest that the binding of the peptide to the ice−water interface is necessary for inhibition of crystal growth. On the basis of these results, we propose that short peptides can be a potent antifreeze agent readily available at low cost.

The more effective retardation by Gly-Pro-Ala-Gly than by Gly-Gly-Ala-Gly shows that the proline residue plays an important role in the kinetic inhibition. The frozen conformation of the peptides within the overgrown ice crystals reveals that the proline residue is pushed away from the growing ice crystal and impedes the incorporation of both the peptide itself and other water molecules into it when either peptide terminal group is stably bound to the ice surface.

Our simulations have focused on only two sequences of tetrapeptides, and the effect of peptide length, sequence, and concentration is of interest. Experiments have shown that longer peptides (8 and 12 residues) might be more effective antifreeze agents. Computer simulations of larger peptides and higher concentrations are feasible but are computationally demanding because of the larger systems necessary. This is particularly true when an investigation of many sequences is of interest. This work has shown, however, that the binding of the peptide to ice is the most important step, and suggests that the sequences can be screened by studying the binding of peptides to the ice, perhaps with implicit solvent. Investigations of this nature are a possible future direction of this work.

The simulations focus on the microscopic growth rate of crystals; i.e., they focus on single crystals. In reality, of course, ice crystals are far more complex. In fact, it is often stated that the recystallization inhibition by antifreeze proteins occurs by the inhibition of grain boundary migration. The simulations do not shed light on how this microscopic retardation is related to grain boundary migration. Mesocopic investigations of crystallization (with input from microscopic simulations) represents another interesting direction of this research.

Acknowledgment. This material is based upon work supported by the United States Department of Agriculture National Research Initiative Program (Grant No. 2006-35503-16998). We acknowledge the National Science Foundation for partial support of this research, under Grant No. CHE-0717569.

References and Notes

(1) DeVries, A. L.; Wohlshlag, D. E. *Science* **1969**, *163*, 1073.
(2) Knight, C. A.; DeVries, A. L.; Oolman, L. D. *Nature* **1984**, *308*, 295.
(3) Knight, C. A.; Cheng, C. C.; DeVries, A. L. *Biophys. J.* **1991**, *59*, 409.
(4) Hansen, T. N. *Proc. Natl. Acad. Sci. U.S.A.* **1992**, *89*, 8953.
(5) Yeh, Y.; Feeney, R. E. *Chem. Rev.* **1996**, *96*, 601.
(6) Knight, C. A. *Nature* **2000**, *406*, 249.

(7) Wierzbicki, A.; Dalal, P.; Cheatham, T. E., III; Knickelbein, J. E.; Haymet, A. D. J.; Madura, J. D. *Biophys. J.* **2007**, *93*, 1442.

(8) Sidebottom, C.; Buckley, S.; Pudney, P.; Twigg, S.; Jarman, C.; Holt, C.; Telford, J.; McArthur, A.; Worrall, D.; Hubbard, R.; et al. *Nature* **2000**, *406*, 256.

(9) Damodaran, S. *J. Agric. Food Chem.* **2007**, *55*, 10918.

(10) Carignano, M. A.; Shepson, P. B.; Szleifer, I. *Mol. Phys.* **2005**, *103*, 2957.

(11) Vrbka, L.; Jungwirth, P. *Phys. Rev. Lett.* **2005**, *95*, 148501.

(12) Nada, H.; Furukawa, Y. *J. Cryst. Growth* **2005**, *283*, 242.

(13) Kim, J. S.; Yethiraj, A. *J. Chem. Phys.* **2008**, *129*, 124504.

(14) Nada, H.; Furukawa, Y. *J. Phys. Chem. B* **2008**, *112*, 7111.

(15) Troitzsch, R. Z.; Vass, H.; Hossack, W. J.; Martyna, G. J.; Crain, J. *J. Phys. Chem. B* **2008**, *112*, 4290.

(16) Hayward, J. A.; Reimers, J. R. *J. Chem. Phys.* **1997**, *106*, 1518.

(17) Lindahl, E.; Hess, B.; van der Spoel, D. *J. Mol. Mod.* **2001**, *7*, 306.

(18) van der Spoel, D.; Lindahl, E.; Hess, B.; Groenhof, G.; Mark, A. E.; Berendsen, H. J. C. *J. Comput. Chem.* **2005**, *26*, 1701.

(19) Berendsen, H. J. C.; Postma, J. P. M.; van Gunsteren, W. F.; DiNola, A.; Haak, J. R. *J. Chem. Phys.* **1984**, *81*, 3684.

(20) Miyamoto, S.; Kollman, P. A. *J. Comput. Chem.* **1992**, *13*, 952.

(21) Darden, T.; York, D.; Pedersen, L. *J. Chem. Phys.* **1993**, *98*, 10089.

(22) Essmann, U.; Perera, L.; Berkowitz, M. L.; Darden, T.; Lee, H.; Pedersen, L. G. *J. Chem. Phys.* **1995**, *103*, 8577.

(23) Mahoney, M. W.; Jorgensen, W. L. *J. Chem. Phys.* **2000**, *112*, 8910.

(24) Vega, C.; Sanz, E.; Abascal, J. L. F. *J. Chem. Phys.* **2005**, *122*, 114507.

(25) Jorgensen, W. L.; Chandrasekhar, J.; Madura, J. D.; Impey, R. W.; Klein, M. L. *J. Chem. Phys.* **1983**, *79*, 926.

(26) Berendsen, H. J. C.; Grigera, J. R.; Straatsma, T. P. *J. Phys. Chem.* **1987**, *91*, 6269.

(27) Jorgensen, W. L.; Maxwell, D. S.; Tirado-Rives, J. *J. Am. Chem. Soc.* **1996**, *118*, 11225.

(28) Kaminski, G. A.; Friesner, R. A.; Tirado-Rives, J.; Jorgensen, W. L. *J. Phys. Chem. B* **2001**, *105*, 6474.

(29) Bauerecker, S.; Ulbig, P.; Buch, V.; Vrbka, L.; Jungwirth, P. *J. Phys. Chem. C* **2008**, *112*, 7631.

(30) Hallett, J. *J. Atmos. Sci.* **1964**, *21*, 671.

(31) Pruppacher, H. R. *J. Chem. Phys.* **1967**, *47*, 1807.

(32) Fernández, R. G.; Abascal, J. L. F.; Vega, C. *J. Chem. Phys.* **2006**, *124*, 144506.

(33) Humphrey, W.; Dalke, A.; Schulten, K. *J. Mol. Graphics* **1996**, *14*, 33.

(34) Pruppacher, H. R. and Klett, J. D. *Microphysics of clouds and precipitation*; D. Reidel Publishing Co.: Hingham, MA, 1978).

JP8110748